

COMPARATIVE STUDY OF FLOW AND HEAT TRANSFER PERIODIC BOUNDARY CONDITIONS

M. Quispe, J. Cadafalch, M. Costa, M. Soria

Centre Tecnològic de Transferència de Calor (CTTC)
Lab. de Termodinàmica i Energètica, Universitat Politècnica de Catalunya (UPC)
ETSEIT, C/Colom 11, 08222 Terrassa, Spain
e-mail: marcos@labtie.mmt.upc.es, web page: <http://www.upc.es/lte>

Key words: Periodic Boundary Conditions, Numerical Errors.

Abstract. *In this paper the comparative study of three periodic boundary conditions formulations will be studied. The results are obtained using the finite-volume method. The discretized governing equations is solved in a segregated manner using the SIMPLEC algorithm. The geometry is discretized with structured cartesian staggered grids. For the comparative study, a benchmark case will be solved. The domain is formed by two parallel plates to which fins are attached in a staggered fashion. Stream-wise periodic variation of the cross-sectional area causes the flow and temperature fields to repeat periodically after a certain developing length. A mesh refinement study and the generalized Richardson extrapolation have been adopted to evaluate the errors and the order of accuracy of each formulation.*

1 INTRODUCTION

Periodic flow and heat transfer behavior appears in many engineering problems of interest, such as compact heat exchangers [7], parallel plate channels with fins placed on the opposite walls [6], transparent insulation covers with honeycomb type structures [8] and electronic equipment cooling [5]. The characteristics of these systems allow to reduce the calculation domains to the zones where the periodicity takes place instead of solving the whole physical domain. Therefore, both CPU time and the required memory for the system modeling are dramatically reduced. Many works are published about this topic. In most of them the periodic boundary conditions are imposed transferring the information of the variables at the outlet periodic boundaries to the inlet ones and vice versa ([6], [7]).

The proper periodic boundary conditions may depend on the studied physical phenomena. Therefore, before solving any problem with periodic flow or heat transfer phenomena a good understanding of the formulation is necessary. Otherwise, the numerical solutions could not represent the real physical behavior.

This paper is focused on the comparison of different formulations for the periodicity treatment based on the finite volume method. Three formulations are considered:

- a) Direct Interpolation Formulation (DIF): Dirichlet boundary conditions in the periodic boundary are fixed for all the dependent variables by means of lagrangian interpolations from the values calculated in the corresponding periodic zone.
- b) Exact Position Formulation (EPF): the values of each dependent variable in the calculation nodes of the periodic boundary are directly transferred from the corresponding nodes in the periodic zone. Some of these nodes are placed inside the domain forming a false boundary.
- c) Conservative Treatment Formulation (CTF): The boundary values at the periodic boundary are calculated forcing the physical fluxes (i.e. mass, momentum and heat fluxes) through the periodic boundary to be equal to the flux to the corresponding section in the periodic zone. This formulation is based on the conservative interpolation schemes used in the multi-block method ([1], [2]).

Numerical details on the implementation of each kind of formulation are described and discussed.

Although a two-dimensional description is given here in order to explain the different formulations used in a clear way, all results hereafter presented can be extrapolated to three-dimensional problems. The results are obtained using the finite-volume method. The discretized governing equations are solved in a segregated manner using the SIMPLEC algorithm. The geometry is discretized with structured cartesian staggered grids.

For the comparative study, a two dimensional incompressible flow through isothermal finned plates [6] is solved using the three periodic formulations. In this case the flow is expected to attain, a periodic fully developed regime, in which the velocity field repeats

itself from module to module with inverted symmetry. The errors and the order of accuracy of the numerical solutions for each formulation have been calculated and compared giving criteria about the suitability of each formulation. Details about the CPU time requirements for each formulation are also given.

2 BENCHMARK PROBLEM

The numerical work described by Kelkar et al. [6] has been chosen as benchmark problem. The geometry considered consist of equally spaced transverse fins that are located in a staggered arrangement on two isotherm walls of a channel, see Figure (1). The fins have the height G which provides a partial blockage of the channel width H . The blockage tends to increase the flow velocity and causes deflection of the main flow so that impingement on one of the walls is created. Since the geometry contains identical geometric modules, the flow is expected to attain, after a short entrance regime, a periodic fully developed regime, in which the velocity field repeats itself from module to module. The flows in the half-modules ABCD and DCEF would exhibit inverted symmetry. Thus, it is possible to confine the computation to the half-module ABCD. The flow is assumed to be laminar, two-dimensional and fluid properties to be constant.

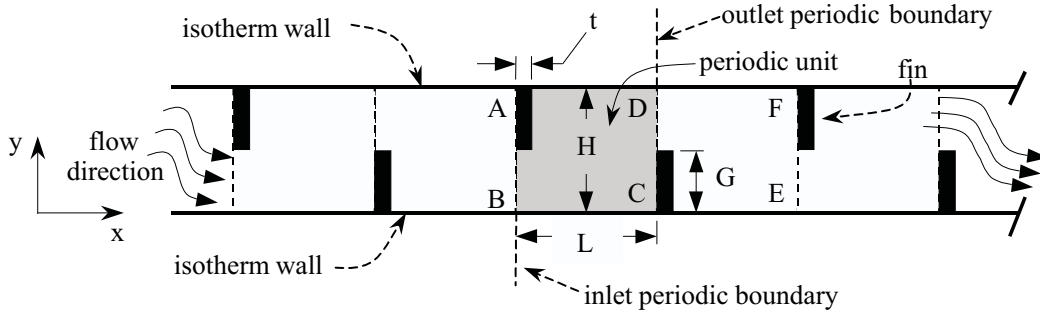


Figure 1: Geometry of the benchmark problem.

The primary issue of concern for any periodic boundary condition formulation is to choose a proper “periodic unit”. Figure (2) shows the discretized “periodic unit” for benchmark problem. It is important to point out that difference between “periodic unit” and “numerical domain”.

The “numerical domain” accounts for the periodic zone and on additional zone of the outlet. According to the nomenclature used in the multi-block method, this zone will be called “overlapping zone”. At least two control volumes (in the flow direction) are necessary in this zone. Otherwise convergence problem may occur.

Boundary conditions in the inlet and outlet periodic boundary will be fixed for the velocity field, the temperature and pressure. These boundary conditions must take into account out of the inverted periodicity of the flow but also the pressure drop and the temperature increase because of the heat exchange within the module, see Table 1.

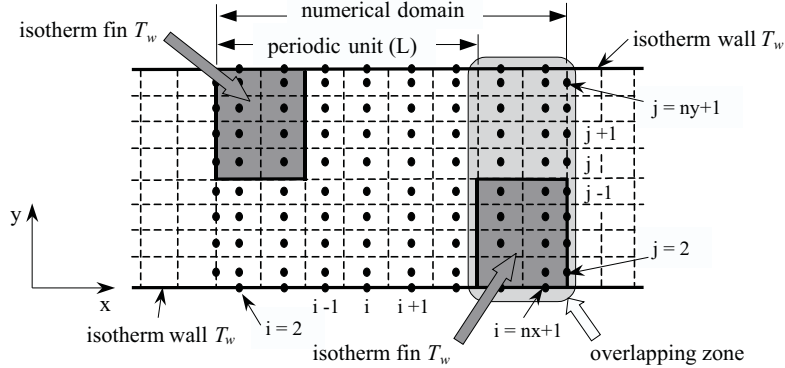


Figure 2: Illustration of the “numerical domain”.

VARIABLE	BOUNDARY CONDITION
Velocity	$U(0, y) = U(L, H - y)$ $V(0, y) = -V(L, H - y)$
Temperature	$[T(0, y) - T_w] / [T_b(0) - T_w] =$ $[T(L, H - y) - T_w] / [T_b(L) - T_w]$
Pressure	$P(x, y) = -\beta x + P^*(x, y)$

Table 1: Boundary condition for the benchmark problem.

The pressure drop in the module is consider by means of the coefficient β and the respective distance between periodic positions. Details on the physical meaning of this case can be found in Kelkar et al. [6].

3 NUMERICAL FORMULATION

Three different numerical formulations are used in this work for the treatment of the boundary conditions using the finite-volume method with a staggered grid arrangement. Hereafter a description of each formulation is given. Details about the implementation of them in the code are pointed out.

3.1 Direct Interpolation Formulation (DIF)

Dirichlet boundary conditions in the periodic boundary are fixed for the velocity field and the temperature by means of interpolations from the values calculated in the corresponding periodic zone. As a staggered grid arrangement is used, the velocity component in the normal direction to the periodic boundary is directly transferred from outlet to inlet periodic nodes and vice versa, see Figure (3-a). On the other hand, both the periodic temperature, Figure (4-a), and the tangential velocity components, Figure (3-b), are interpolated by means of lagrangian interpolations (third accurate bi-quadratic interpo-

lation have been used) in order to preserve the overall order accuracy of the numerical solution [4].

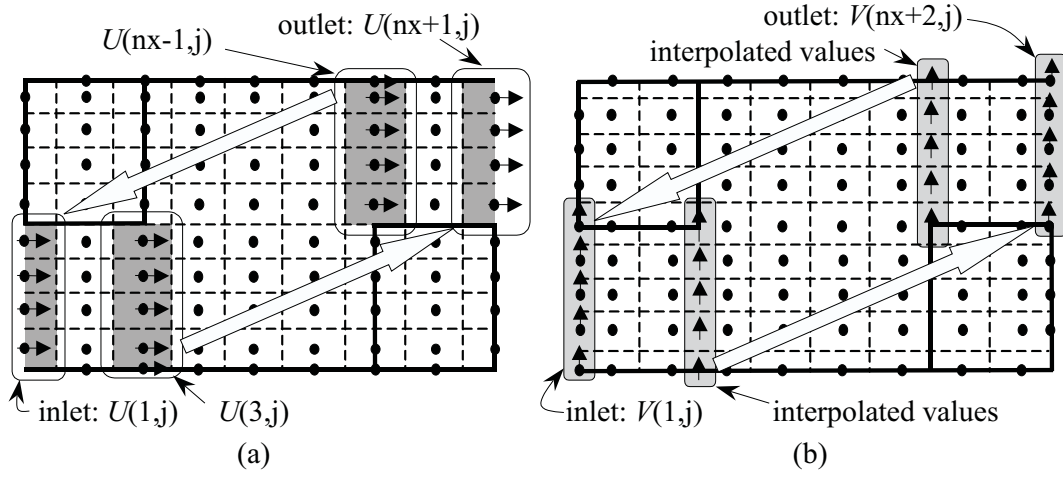


Figure 3: Treatment of U and V for DIF formulation. (a) Staggered grid in horizontal direction, (b) Staggered grid in vertical direction.

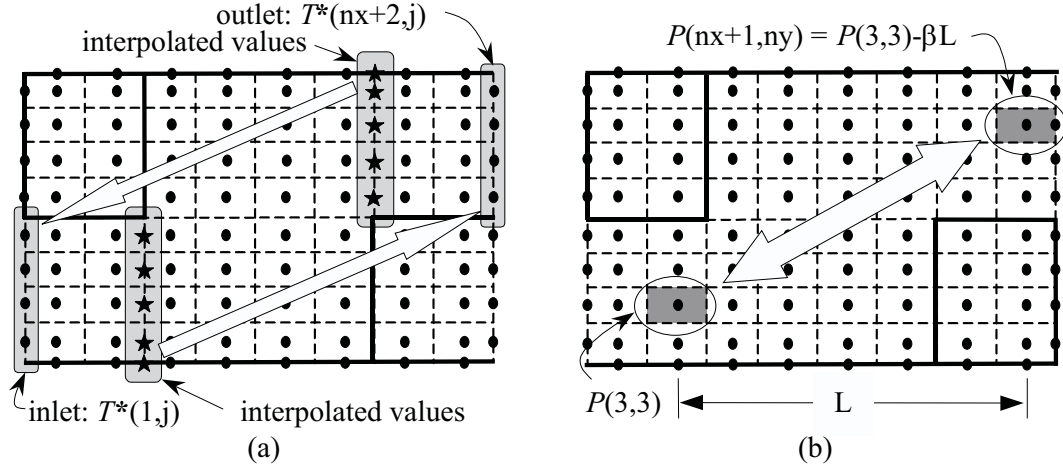


Figure 4: Treatment of T^* and P for DIF formulation on main grid.

The periodic calculation for the pressure, Figure (4-b), has been fixed at just one internal node next to the periodic boundary. Whatever control volume at the control volumes row next to the periodic boundary could be arbitrary chosen.

This formulation does not require any modification on the calculation of the algebraic coefficients of the discretized equations of the internal control volumes a part from the

treatment of the pressure at the chosen node. Therefore, the periodicity can be almost fully imposed dealing with the equations of the periodic boundary.

3.2 Exact Position Formulation (EPF)

The values for all the variables at the periodic zone are directly transferred from corresponding nodes, as it is show in Figures (5) and (6).

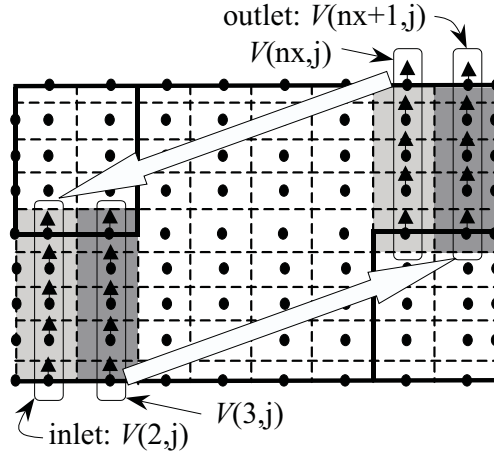


Figure 5: Treatment of V for EPF formulation on staggered grid in vertical direction.

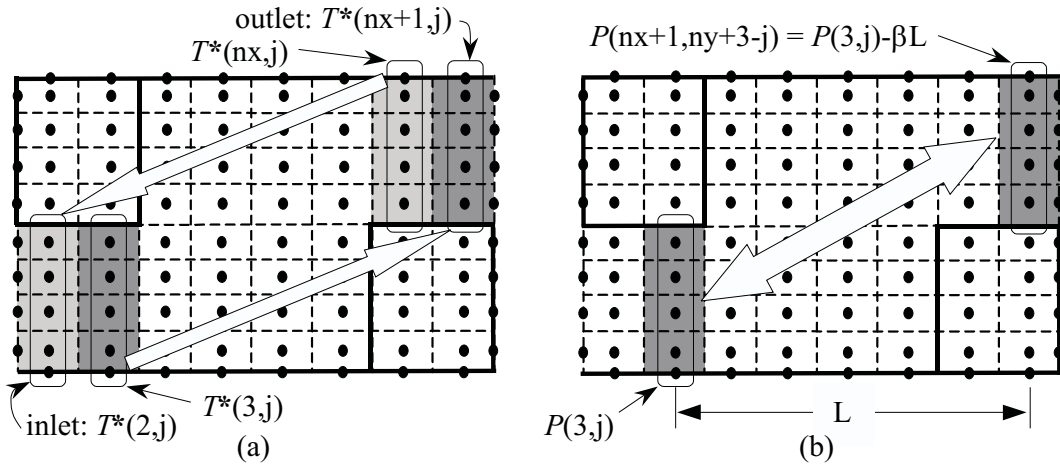


Figure 6: Treatment of T^* and P for EPF formulation on main grid.

The nodes for the velocity component normal to the periodic boundary are placed at the boundary itself. On the other hand, nodes for the periodic temperature and the

tangential boundary are placed inside the domain at row of control volumes close to the boundary. Therefore, the calculation domain is reduced (with one row of control volumes less for the outlet and inlet periodic boundary). In this formulation the periodicity of the pressure field must be imposed at all the control volumes that belong the these control volumes rows close to the periodic boundaries.

The corresponding algebraic equations are similar to those obtained when cyclic solvers for the periodic treatment are used [7] transferring the periodic information in on explicit manner instead of solving at within an implicit procedure.

3.3 Conservative Treatment Formulation (CTF)

The boundary values at the periodic boundary are calculated forcing the physical fluxes (i.e. mass, momentum and heat fluxes) through the periodic boundary to be equal to the flux through the corresponding section in the periodic zone, see Figure (7). This formulation is based on the conservative interpolation schemes used in the multi-block method ([1], [2]). The pressure is resolved as in the direct interpolation formulation (DIF), imposing the periodicity at only one control volume at the control volume row close to the periodic boundary.

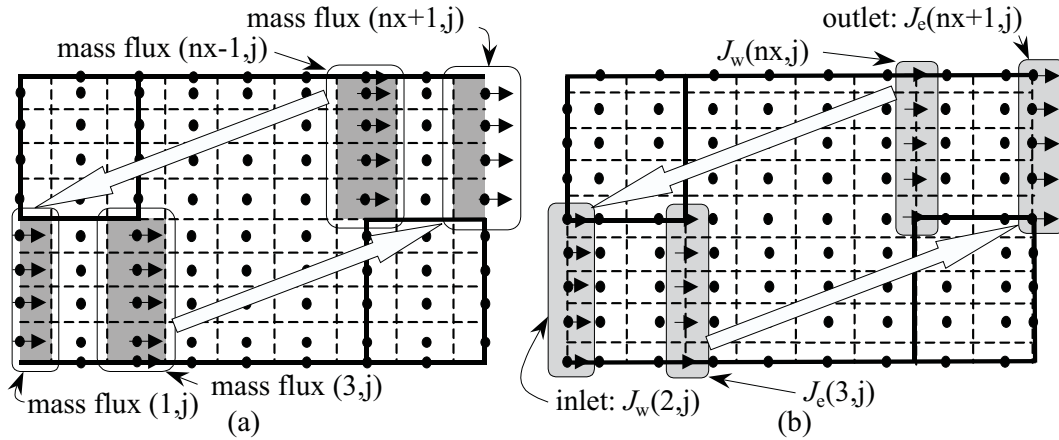


Figure 7: Treatment of mass flux and J for CTF formulation. (a) Staggered grid in horizontal direction, (b) Staggered grid in vertical direction.

4 EVALUATION OF THE ERROR AND ORDER OF ACCURACY OF THE NUMERICAL SOLUTION

In order to evaluate the quality of the numerical solutions, the numerical error ed and the order of accuracy p are estimated using a post-processing tool described in detail in [1]. An h -refinement treatment is adopted. The problem is solved on different meshes related by a mesh ratio r (in this work $r = 2$ and six levels of refinement are studied).

According to the Richardson extrapolation [3], with three solutions of a problem (ϕ_1 , ϕ_2 and ϕ_3) obtained on the grids $h_1 = h$ (fine grid), $h_2 = rh$ (middle grid) and $h_3 = r^2h$ (coarse grid), the order of accuracy of the numerical solution can be determined by the following equation when the assumptions of smoothness and monotone error convergence in the mesh spacing apply:

$$p = \frac{\ln(\frac{\phi_2 - \phi_3}{\phi_1 - \phi_2})}{\ln(r)} \quad (1)$$

A map of the estimated order of accuracy is calculated with three consecutive mesh levels.

A single grid independent solution is also carried out. The “exact” or reference solution is considered, and maps of errors for each refinement level are obtained. Usually, a grid-independent numerical solution is taken as a reference or “exact” solution. Thus, a grid-independent solution has been calculated for all the testing problems used in this article. They have been considered the “exact” or reference solution for the error studies. Then, the numerical normalized error maps of the same test problems solved on different grids or numerical schemes have been carried out by:

$$ed(x) = | \phi^*(x) - \phi_E^*(x) | \quad (2)$$

where $\phi^*(x)$ is the normalized solution, $\phi_E^*(x)$ is the normalized “exact” solution, and x stands for the coordinates of the discretized nodes of the solution studied (position vector).

In both the error map and the numerical accuracy map, as the compared meshes do not have coinciding nodes, it has been necessary to interpolate information from the solutions. Bi-quadratic interpolations have always been used so as not to introduce uncertainties in the post-processing study.

The average p and the average error ed have been adopted as global estimators of the global order of accuracy and the global numerical error. As the calculation of p requires three consecutive mesh levels, and the h -refinement treatment has been carried out on six levels, only three p estimators are calculated. On the other hand, the numerical error estimations is evaluated for each level of refinement.

This post-processing tool has to be applied segregatedly on all variables of the problem.

5 RESULTS AND DISCUSSIONS

5.1 Study of the error

The evolution of the numerical errors ed was analyzed using uniform two-dimensional grid size of $(n+4) \times n$ (with six refinement levels, $n = 6, 12, 24, 48, 96$ and 192). This analysis has been carried out for all the variables. The required grid-independent solutions have been obtained on a 196×192 uniform grid using SMART scheme and CTF formulation.

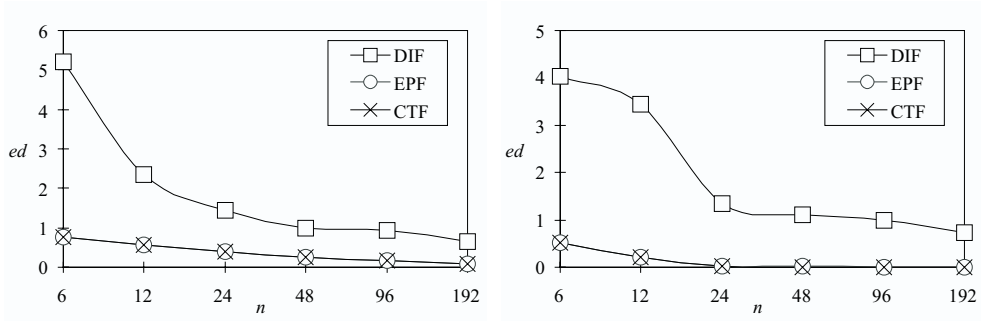


Figure 8: Evolution of the error for U_d . Left: UDS, Right: SMART.

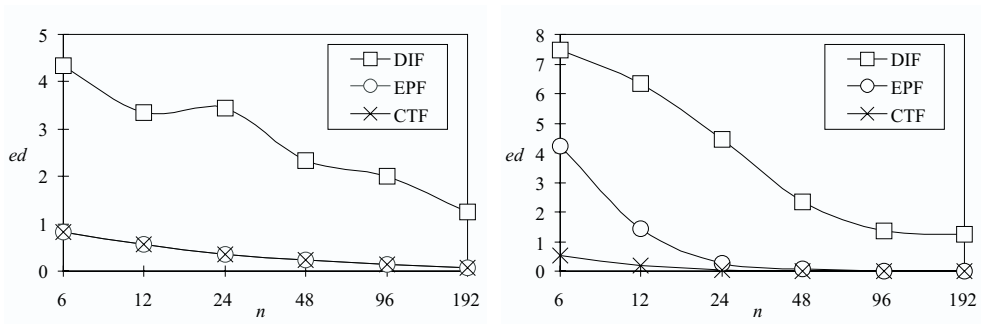


Figure 9: Evolution of the error for V_d . Left: UDS, Right: SMART.

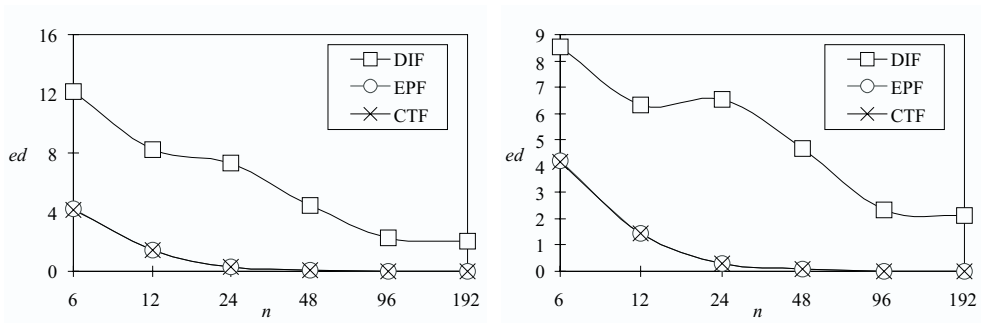


Figure 10: Evolution of the error for T_d . Left: UDS, Right: SMART.

The control of numerical convergence for a time step computation is done obtaining the normalized residual of each equation that is solved. The numerical convergence is considered achieved when the residual of all the variables and the overall normalized mass imbalance are below of the convergence prescribed value $\varepsilon = 1.0 \times 10^{-6}$.

The evolution of the error on EPF and CTF formulations are very good in all variables, only some disagreements appear for the coarse grids ($n = 6$), where the numerical solution is far from the grid independent solution. On the other hand, the values of the DIF

formulation are higher than the values of the EPF and CTF, as it can be seen in Figures (8), (9) and (10).

It is outstanding that the results obtained with EPF and CTF are similar when the UDS scheme is used for U_d and V_d analysis. However, when the SMART scheme was used, it was observed differences between EPF and CTF formulations, although these differences are small, computations indicated a maximum difference of 1.16% for a grid size of 196x192 on U_d study, and of 11.32% on V_d analysis for a grid size of 10x6. In the T_d error results with EPF and CTF there exists a maximum difference for a grid size of 0.05% when the UDS scheme is used and a value of 0.06% for a grid size of 10x6 when the SMART scheme is used.

5.2 Study of the order of accuracy

Tables (2), (3) and (4) show information about the evolution of accuracy of the numerical solution of the U_d , V_d and T_d variables, using three consecutive meshes and using a post-processing tool based on the Richardson extrapolation [3].

The comparison between the different levels of refinement involves the hypothesis of equality of the grid spacing. Since control volumes placed on fin zones are different to control volumes placed between fins, some differences in the values of the estimated order of accuracy could be expected a priori. However, good agreement is always achieved (mainly on CTF and EPF formulation) between the values calculated with UDS and SMART studies. All of them are also expected values: around 1 when the convective terms are modeled by means of the first order UDS, and around 2 for the cases with the high order SMART scheme. The results with both the CTF and EPF formulations are similar when UDS is used over U_d and V_d analysis. With the SMART scheme there exist minimum differences.

With the DIF formulation, the order of accuracy is not good, although the values are between the limits expected in the SMART scheme.

Grid			p					
			UDS			SMART		
Coarse	Middle	Fine	CTF	EPF	DIF	CTF	EPF	DIF
10x6	16x12	28x24	0.6986	0.6985	-0.3423	0.7443	0.7139	-0.1125
16x12	28x24	52x48	0.4231	0.4231	0.0126	2.7710	2.7900	0.4512
28x24	52x48	100x96	0.5729	0.5729	0.2543	2.3861	2.4437	1.1256
52x48	100x96	196x192	0.6874	0.6874	0.3321	1.9813	1.6599	1.0345

Table 2: Average p value for the U_d field ($Re = 100$).

Grid			p					
			UDS			SMART		
Coarse	Middle	Fine	CTF	EPF	DIF	CTF	EPF	DIF
10x6	16x12	28x24	-0.176	-0.1761	-0.2452	0.9507	0.9436	-0.7344
16x12	28x24	52x48	0.5086	0.5087	0.05245	2.3438	2.3230	-0.6345
28x24	52x48	100x96	0.5953	0.5953	0.1249	1.8015	1.8325	0.8345
52x48	100x96	196x192	0.6670	0.6669	0.3834	1.7306	1.6974	1.1053

Table 3: Average p value for the V_d field ($Re = 100$).

Grid			p					
			UDS			SMART		
Coarse	Middle	Fine	CTF	EPF	DIF	CTF	EPF	DIF
10x6	16x12	28x24	0.2474	0.1579	-0.7356	0.4630	0.4358	-0.6346
16x12	28x24	52x48	0.6127	0.6454	0.02345	1.9507	1.9719	0.03456
28x24	52x48	100x96	0.5130	0.5229	0.0456	2.2206	2.2790	0.34566
52x48	100x96	196x192	0.6150	0.6147	0.3456	2.3356	2.4223	1.2456

Table 4: Average p value for the T_d field ($Re = 100$).

5.3 Study of ff , lc , and Nu

The plot of the friction factor ff versus n can be seen in Figure (11). The maximum difference between values of ff when SMART scheme is used (with EPF and CTF formulations) is 0.437 % in a grid size of 196x192. For UDS scheme this difference is zero, in other words, there always exists the same results in any grid size. The values obtained with DIF formulation present a difference of 36.48 % for a grid size of 196x192 with UDS scheme, and of 12.41 % with SMART scheme, in relation to CTF formulation.

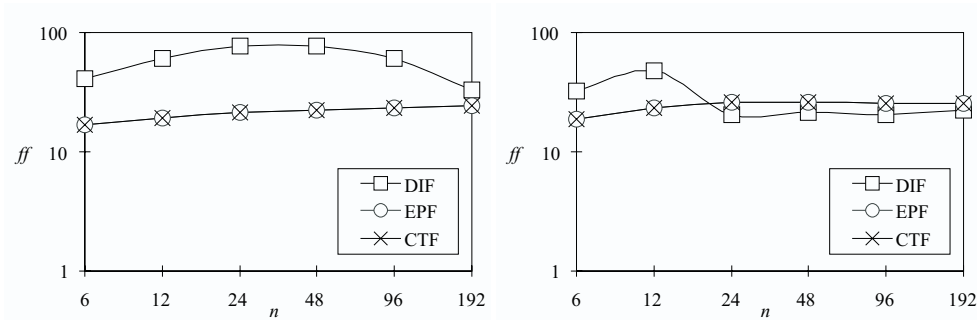


Figure 11: Evolution of the friction factor. Left: UDS, Right: SMART.

The comparisons of the maximum value of normalized stream function lc are presented

in Figure (12). Based on these comparisons, the numerical treatment of DIF formulation generates more error on the lc than that with CTF and EPF formulations. The difference between DIF and CTF formulation for grid size of 196x192 is 26.21 % with UDS scheme, and 19.43 % with SMART scheme.

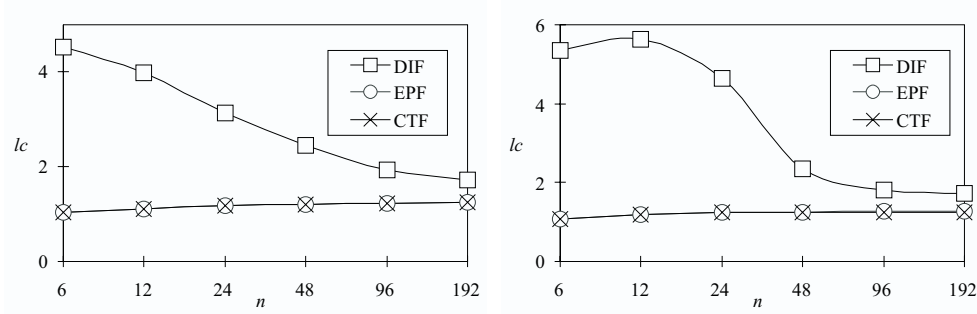


Figure 12: Evolution of the maximum line current. Left: UDS, Right: SMART.

The results for Nusselt number are displayed in Figure (13). Similar conclusions obtained in ff and lc analysis are found in Nu results. The difference was 28.38 % in a grid size of 196x192 with UDS and 24.72 % with SMART scheme when DIF was compared with CTF formulation.

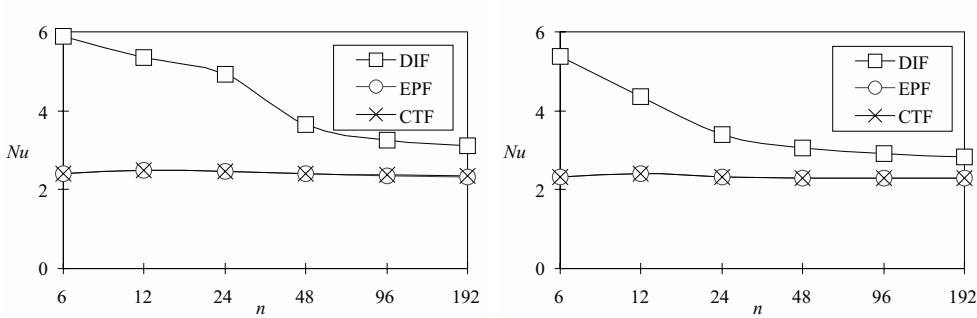


Figure 13: Evolution of the Nusselt number. Left: UDS, Right: SMART.

The cost computational required similar CPU time for CTF and EPF formulations. For example, when a grid size of 96x92 was used with SMART scheme, CTF formulation required 5.4 hour and EPF formulation need 5.1 hour. In the same conditions, DIF formulation need 8.3 hour of CPU time.

The results of the ff versus Re are presented, using an array of 96x92 with irregular spaced grid, SMART scheme and CTF formulation. In Figure (14), these values are compared with results obtained by Kelkar et al. [6]. It was observed that the maximum difference in friction factor was 8,63% at $Re = 100$.

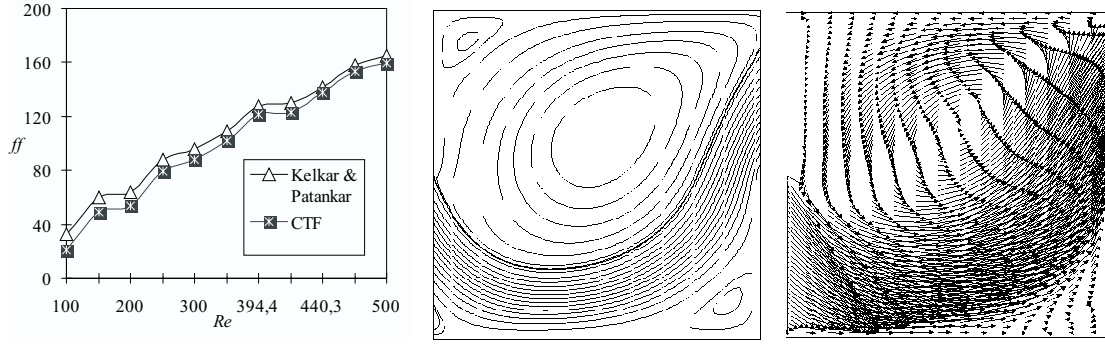


Figure 14: Left: Evolution of the friction factor. The values obtained with CTF formulation are comparing to the Kelkar et.al [6] results. Center and Right: Streamline and velocity vectors for $Re = 100$.

6 CONCLUSIONS

The numerical results obtained show that the values of both exact position formulation and conservative treatment formulation are very good and require similar CPU times. The most important differences between them are found in the way of introducing the periodic formulation in the algebraic equations. As the former uses a false boundary involving nodes contained inside the domain, the algebraic equations in these nodes need to be changed, while for the latter only the algebraic equations of the boundary nodes need to be modified. On the other hand, the formulation based on direct interpolations introduces imbalances of the physical quantities increasing the CPU time and introducing inaccuracies in the numerical solution even when fine meshes are used.

This work demonstrates that exact position formulation and conservative treatment formulation preserves the order of numerical accuracy and does not introduce additional uncertainty in the numerical solution. On the other hand, the results with exact position formulation and conservative treatment formulation are the same when UDS is used over U_d and V_d fields comparing to the SMART results where it exists little differences.

7 ACKNOWLEDGEMENTS

This work has been financially supported by the Comisión Interministerial de Ciencia y Tecnología, Spain (project TIC99-0770).

Nomenclature

β	overall rate of pressure drop	r	mesh ration in the h -refinement
ed	discretization error	Re	Reynolds number
ff	friction factor	t	thickness of the fins
G	height of the fins	T	temperature
H	width of the channel	T^*	periodic temperature
J	momentum flux through the c.v. faces	T_b	bulk temperature of the fluid

L	periodic longitude	T_d	dimensionless temperature: $(T - T_w)/(T_b - T_w)$
lc	stream function normalized		
n	refinement level	T_w	constant temperature of the walls
Nu	Nusselt number	U, V	cartesian velocity components
nx	number of c.v. in x direction	U_d, V_d	dimensionless velocities: $U/[(\int U dy)/H], V/[(\int U dy)/H]$
ny	number of c.v. in y direction		
p	order of accuracy	x, y	cartesian coordinates
P	static pressure		
P^*	periodic part of pressure		

References

- [1] J. Cadafalch, A. Oliva, C. D. Pérez Segarra, M. Costa and J. Salom, “Comparative study of conservative and nonconservative interpolation schemes for the domain decomposition method on laminar incompressible flows”, *Numerical Heat Transfer, Part B, Fundamentals*, Vol. **35**, 113-136 (1999).
- [2] J. Cadafalch, C. D. Pérez Segarra, M. Soria and A. Oliva, “Fully conservative multi-block method for the resolution of turbulent incompressible flows”, *Proceedings of the Fourth European Computational Fluid Dynamics Conference*, Vol. **I**, Part. 2, 1234-1239. John Wiley and Sons, Athens, Greece, October (1998).
- [3] I. Celik and Vei-Ming Zhang, “Calculation of numerical uncertainty using Richardson extrapolation: Application to some simple turbulent flow calculations”, *Journal of Fluids Engineering*, Vol. **117**, 439-445 (1995).
- [4] G. Chesshire, W. D. Henshaw, “A Scheme for conservative interpolation on overlapping grids”, *SIAM J. of Scientific Computing*, Vol. **15**, No. 4, 819-45 (1994).
- [5] K. M. Kelkar and D. Choudhury, “Numerical prediction of periodically fully developed natural convection in a vertical channel with surface mounted heat generating blocks”, *Int. J. Heat Mass Transfer*, Vol. **36**, No. 5, 1133-1145 (1992).
- [6] K. M. Kelkar and S. V. Patankar, “Numerical prediction of flow and heat transfer in a parallel plate channel with staggered fins”, *Journal of Heat Transfer*, Vol. **109**, 25-30 (1987).
- [7] S. V. Patankar, C. H. Liu and E. M. Sparrow, “Fully developed flow and Heat transfer in ducts having streamwise-periodic variations of cross-sectional area”, *Journal of Heat Transfer*, Vol. **99**, 180-186 (1977).
- [8] H. Schweiger, A. Oliva, M. Costa and C. D. Pérez Segarra, “Numerical experiments on laminar natural convection in rectangular cavities with and without honeycomb-structures”, *International Journal of Numerical Methods for Heat for Heat and Fluid Flow*, Vol. **5**, No. 5, 423-443 (1995).